Tranverse magnetotunneling in $Al_xGa_{1-x}As$ capacitors. I. Angular dependence

T. W. Hickmott
IBM Research Division, T. J. Watson Research Center, Yorktown Heights, New York, 10598
(Received 18 May 1989)

The angular dependence of transverse magnetotunneling from an accumulation layer on n^--type GaAs has been studied in four n^--type GaAs–$Al_xGa_{1-x}As$–n^+-type GaAs capacitors with values of substrate doping N_S between 1.2×10^{15} and 7×10^{15} cm^{-3}. At high current densities, when tunneling is from excited subbands of the two-dimensional electron gas (2DEG) of the accumulation layer, there is a remarkably sharp angular dependence of the voltage required for a given tunnel current J when J is perpendicular to the magnetic field B. The angular width of the dependence is $\sim2°$ and is independent of N_S. The magnitude of the angular dependence is greatest for low N_S. The angular dependence is observed when the diameter of the cyclotron orbit of electrons in the 2DEG is less than the width of the accumulation layer at the Fermi energy, resulting in a reduction of the number of electrons with a velocity component normal to the n^--type GaAs/$Al_xGa_{1-x}As$ interface that are available for tunneling.

INTRODUCTION

The effect of a magnetic field B on tunneling in single-barrier[1–12] or multibarrier[13–21] heterostructures has been reported in a number of recent papers. For longitudinal magnetotunneling, B is perpendicular to the heterostructure and B is parallel to J, where J is the tunnel current density. If a two-dimensional electron gas (2DEG) is present in the heterostructure, tunnel currents reflect the presence of Landau levels in the 2DEG whose energy separation and population are proportional to $B\cos\theta$, where θ is the angle between B and the normal to the 2DEG.[2,10,13] The change in the magnitude of J with B is relatively small. For transverse magnetotunneling, B is parallel to the heterostructure interfaces or 2DEG, and is perpendicular to J. Landau levels do not form in the 2DEG although bulk Landau levels can be present and can affect tunneling currents.[5–7] In single-barrier heterostructures a decrease in J with increasing B is observed.[1,3–5] In multibarrier heterostructures there is a suppression of negative differential conductivity at high transverse magnetic fields.[14,16,17,19,20] Theoretical analysis of transverse magnetotunneling is complicated by the difficulty in separating the effects of magnetic field and electric field in the Hamiltonian of the 2DEG system.[8,11,15]

The simplest form of the equation for tunneling in the direction z through the barrier of a heterostructure is[22]

$$J=q\int_0^\infty N(E_z)D(E_z)dE_z\ , \tag{1}$$

where q is the electric charge, $N(E_z)$ is the number of electrons impinging on a barrier per cm^2 per second with an energy E_z, and $D(E_z)$ is the transmission probability. Analyses of the effect of the Lorentz force on a tunneling electron in decreasing the tunnel current have generally emphasized the effect of the magnetic field on the transmission coefficient $D(E_z)$.[3,4] The effect of B on the source function $N(E_z)$ has not generally been considered though it was suggested that the sharply peaked angular dependence of magnetotunneling currents at high current densities when θ was varied around 90° is due to the reduction by B of the number of electrons that can tunnel from an accumulation layer.[5] In this paper we present results on the angular dependence of transverse magnetotunneling in a single-barrier heterostructure when θ is close to 90° which show that the effect of B on the source function $N(E_z)$ can drastically change tunnel currents. For samples with low-doped n-type GaAs as the source of electrons, the effect is much larger than the effect of a transverse magnetic field on the transmission coefficient.

EXPERIMENTAL

The samples studied in the present work are n^--type GaAs–$Al_xGa_{1-x}As$–n^+-type GaAs (AlGaAs) capacitors, shown schematically in Fig. 1(a), where x is the mole fraction of AlAs in the dielectric layer. When the gate voltage V_G is greater than the flat-band voltage V_{FB} an accumulation layer forms on the n^--type GaAs substrate. Electrons in the accumulation layer form a degenerate 2DEG whose population is determined primarily by the electric field at the n^--type GaAs/$As_xGa_{1-x}As$ interface. At low temperatures conduction through the $Al_xGa_{1-x}As$ barrier is by tunneling. Longitudinal magnetotunneling and magnetocapacitance curves can be used to determine carrier concentration, energy separation of subbands, and g values of electrons in the accumulation layer.[2,23] Two types of tunneling can be distinguished: (1) direct tunneling in which electrons tunnel from the GaAs substrate through the forbidden band of the $Al_xGa_{1-x}As$ barrier and into the n^+-type GaAs gate, and (2) Fowler-Nordheim (FN) tunneling in which electrons tunnel from the GaAs substrate into the conduction band of the $Al_xGa_{1-x}As$ layer before reaching the GaAs gate. Figure 1(a) corresponds to FN tunneling.

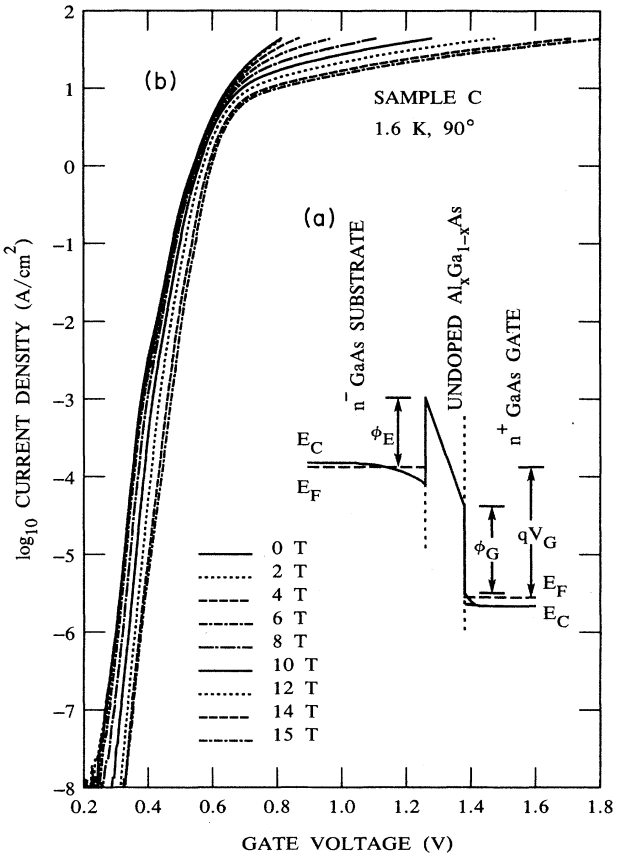

FIG. 1. (a) Schematic energy-band diagram for n-type GaAs undoped $Al_xGa_{1-x}As$–n^+-type GaAs capacitator biased into accumulation. (b) $\log_{10}$ current density vs gate voltage for AlGaAs capacitor for different magnetic fields parallel to the AlGaAs capacitor $\theta=90°$.

For AlGaAs capacitors with comparable values for ϕ_E, the effective barrier height at the n^--type GaAs/$Al_xGa_{1-x}As$ interface, whether direct or FN tunneling occurs depends on the barrier thickness w. For $x\sim0.4$, direct tunneling occurs for $w\lesssim25$ nm, FN tunneling occurs for $w\gtrsim30$ nm. The two modes of tunneling can be distinguished by current-voltage (I-V) curves at low gate voltage. FN tunneling requires $V_G>\phi_G/q$ while direct tunneling currents occur for $0<V_G\leq\phi_G/q$, where ϕ_G is the barrier height at the $Al_xGa_{1-x}As/n^+$-type GaAs interface.

The Fowler-Nordheim tunneling formula is[24–26]

$$\ln\left[\frac{J}{F^2}\right]=\ln B_0-\beta/F\ , \tag{2}$$

where J is the current density in A/cm^2 and F is the field across the insulator in V/cm. B_0 depends on the source function for electrons; β depends primarily on the barrier properties and

$$\beta=\frac{4}{3}\frac{(2m_I)^{1/2}}{q\hbar}\phi_E^{3/2}$$
$$=6.83\times10^7\left[\frac{m_I}{m}\right]^{1/2}\phi_E^{3/2} \tag{3}$$

in V/cm, where m_I is the effective electron mass in the insulator, m is the free electron mass, $\hbar$ is the reduced Planck's constant, and ϕ_E is in electron volts.

Resonant FN tunneling can occur in AlGaAs capacitors due to the perfection of the $Al_xGa_{1-x}As$/GaAs interface.[27] In resonant FN tunneling the I-V characteristics are modulated by interference between electrons transmitted through the $Al_xGa_{1-x}As$ conduction band and electrons that are reflected at the $Al_xGa_{1-x}As/n^+$-type GaAs interface. The effect was first predicted to occur in metal-insulator-metal diodes by Gundlach,[28] and has been observed in metal-oxide-semiconductor (MOS) structures based on silicon,[29–31] and in III-V heterostructures.[27,32]

The angular dependence of transverse magnetotunneling has been studied in four samples whose properties are given in Table I. All samples were grown by molecular-beam epitaxy on ⟨100⟩-oriented n^+-type GaAs wafers. After sample growth Au-Ge-Ni Ohmic contacts were formed on the n^+ substrate and gate, and capacitors of 4.13×10^{-4} cm^2 area were defined by etching a mesa structure. Procedures for measuring I-V and capacitance-voltage (C-V) curves are described elsewhere.[2,33] Magnetic field measurements were made in a superconducting magnet capable of producing 15 T; the sample was immersed in pumped liquid helium to control

TABLE I. Properties of AlGaAs capacitors. N_S is the substrate doping, N_G is the gate doping, w_{cp} is the $Al_xGa_{1-x}As$ thickness derived from C-V curves, ϵ_I is the dielectric constant at 1.6 K, ϕ_G is the activation energy for thermionic emission, x is the AlAs mole fraction of the $Al_xGa_{1-x}As$ barrier layer, V_{FB} is the flat-band voltage, and w_{tn} is the $Al_xGa_{1-x}As$ thickness derived from resonant FN tunneling curves.

Sample	Number	N_S (10^{15} cm^{-3})	N_G (10^{18} cm^{-3})	w_{cp} (nm)	ϵ_I	ϕ_G (eV)	x	V_{FB} (V)	w_{tn} (nm)
A	1332A3	1.7	0.9	21.8	11.2	0.32	0.40	−0.030	
B	432C6	7.0	1.8	20.6	11.5	0.26	0.33	−0.045	
C	834C1,2	1.2	2.0	34.7	11.6	0.24	0.30	0.005	30
D	862A2,4	2.9	2.0	33.2	11.2	0.33	0.40	0.020	27

temperature. The properties of the samples in Table I are derived from *C-V* and *I-V* curves. The sample number is included since the same samples have been studied in earlier work. N_S and N_G, the substrate and gate doping, respectively, are determined by comparing experimental *C-V* curves between 77 and 200 K with calculated *C-V* curves.[33] The thickness w_{cp} is that obtained from *C-V* curves between 77 and 200 K; it depends on the value assumed for the dielectric constant of $Al_xGa_{1-x}As$ which depends, in turn, on the AlAs mole fraction x. The values of dielectric constant are ϵ_I. It is assumed that ϵ_I for $Al_xGa_{1-x}As$ can be extrapolated from the value for GaAs at 300 K, 13.1, and the value of AlAs at 300 K, 10.06. The value of ϵ_I has been corrected for the decrease which occurs at low temperature.[33] The gate barrier height ϕ_G is obtained from analysis of the temperature dependence of *I-V* curves in the temperature region in which thermionic emission dominates. The value of x is derived from the measured value of barrier height and corresponds to the relation ϕ_G (eV)$=(0.77\pm0.02)x$ for the conduction-band discontinuity between GaAs and $Al_xGa_{1-x}As$.[34] The flat-band voltage V_{FB} is determined from structure in either *I-V* or *C-V* curves due to Landau levels in the accumulation layer when a magnetic field is applied perpendicular to an $Al_xGa_{1-x}As$ capacitor. Samples *C* and *D* have negative charge in the undoped-$Al_xGa_{1-x}As$ barrier which shifts V_{FB} from a negative voltage to a small positive value.[33] Samples *A* and *B* are direct tunneling samples; samples *C* and *D* both show resonant FN tunneling in their *I-V* characteristics. The thickness w_{tn} is the value obtained from periodicities in the analysis of resonant FN tunneling.[27,29] From the point of view of its effect on the angular dependence of *I-V* curves, the substrate doping N_S is the most significant parameter since it defines the width of the accumulation layer. N_S varies from 1.2×10^{15} cm^{-3} for sample *C* to 7×10^{15} cm^{-3} for sample *B*.

RESULTS

The most detailed results are given for sample *C* since it shows most strongly the effect of changing the angle around 90° on *I-V* curves. *I-V* curves at 1.6 K as a function of magnetic field *B* for sample *C* are shown in Fig. 1(b). *B* is parallel to the $GaAs/Al_xGa_{1-x}As$ interface. Sample *C* shows resonant FN tunneling;[27,35] at 0 T, there is modulation of *I-V* curves which can be analyzed by the procedures developed by Maserjian *et al.*[29,30] Two effects of *B* are striking in Fig. 1(b); at low biases ($0.22 < V_G < 0.4$ V) the current at fixed V_G is reduced by up to 3 orders of magnitude at 15 T. At high current densities ($J > 10$ A/cm^2) much higher values of V_G are required to reach a given current level when *B* is present. The effects at high values of *J* are closely related to the effects of angle on *I-V* characteristics.

The effect of angle on *I-V* curves of sample *C* is shown in Fig. 2(a). The solid line in Fig. 2(a) is the *I-V* curve for $B=14$ T and $\theta=90°$. The curves that branch off it at high *J* are for different angles of *B* with respect to *J*. Figure 2(b) has an expanded scale for current density but has the same voltage scale as Fig. 2(a). Small changes of angle from 90° markedly affect the *I-V* curves at high current densities but have insignificant effects for current densities below ~1 A/cm^2. The sample holder used for measurements has a resolution and reproducibility of ~0.3°. Also shown in Fig. 2(a) are *I-V* curves at 0 and at 14 T, with **B**||**J**, $\theta=0°$. The effect of *B* on *J* is much smaller in that case; there is a small reduction of *J*, and there is structure due to the effect of Landau levels in the accumulation layer which can be shown by plotting the ratio $J(B)/J(0)$ as a function of V_G.[36]

One way to illustrate the effect of angle on *I-V* curves is shown in Fig. 3. In Fig. 2(b) the horizontal dotted line shows the value of *J* that corresponds to a sample current of 15 mA. In Fig. 3 the voltage for 15 mA when *B* is 14 T is plotted as a function of angle for four samples. The lines marked V_0 in Fig. 3 show the value of V_G for $I=15$ mA when $\theta=0°$ for the different samples. The lines connecting points in Fig. 3 are for clarity; they have no theoretical significance. All four samples show a peak in

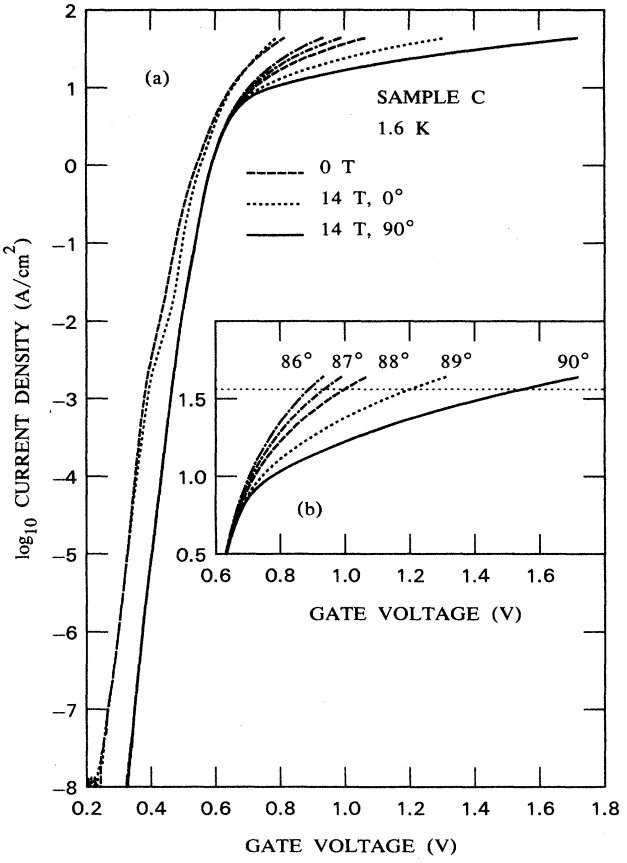

FIG. 2. (a) $\log_{10}$ current density vs gate voltage for AlGaAs capacitor for different sample angles close to 90°. $B=14$ T. Curves are also shown for $B=14$ T, $\theta=0°$, and for $B=0$ T. (b) $\log_{10}$ current density vs gate voltage with an expanded current density scale, for different sample angles. Dotted line shows current density equivalent to a sample current of 15 mA. $B=14$ T.

V_G in 15 mA, V_M. It is remarkable how sharp the peak is. The full width at half maximum (FWHM) for the curves is $\sim 2°$ and is essentially the same for all four samples in spite of the large differences in the magnitude of V_M for different samples.

The value of V_M depends on magnetic field. In Fig. 4(a) V_M for three samples is plotted as a function of B; in Fig. 4(b), $V_M - V_0$ is plotted as a function of B^2 for samples A and C. The lines in Fig. 4(b) are least-squares fits of the data points at high values of B. The dependence of V_M on B is parabolic for the two lightly doped samples and is perhaps becoming so for sample D above 13 T.

The method of displaying data in Fig. 3 is convenient for showing the sharply peaked angular dependence of I-V curves but it has no theoretical basis. In addition the choice of 15 mA is arbitrary; any value of I in the high current tunneling regime gives essentially the same result. Since the I-V curves at high current densities in Figs. 1 and 2 are what would be observed if a large series resistance were present, an alternate way of plotting the data is to calculate a series resistance dV/dI in the high current regime. In Fig. 5 the series resistance for sample A when $I=15$ mA is plotted as a function of angle for $78° \leq \theta \leq 90°$ and for different magnetic fields. The plot is as sharply peaked as the angular dependence of V_M shown in Fig. 3; the half-width of angular dependence is $\sim 1°$ as in Fig. 3. The ordering of points at 89° is not in strict order of B in Fig. 5 while the points at 90° are. The latter were taken with a single unchanged setting of the sample holder. The points at other angles required setting of the angle at each magnetic field. The discrepancy in sequence reflects uncertainties in adjusting the angle and the steep angular dependence of effective series resistance. Either plotting data as in Fig. 3 or in Fig. 5 shows the same peaked angular dependence of I-V curves around 90°, with a half-width independent of B and independent of sample characteristics. It appears to be solely a function of the angular alignment between B and the sample.

The magnitude of suppression of current by a transverse magnetic field can be estimated for sample C by using the FN analysis of Eq. (2). In Eq. (2), $\ln(J/F^2)$ is plotted as a function of $1/F$, where F is the field at the substrate. As shown in Fig. 1(a) the applied voltage is divided into band bending in substrate and gate, and the voltage across the undoped $Al_xGa_{1-x}As$ which determines F. The C-V curve of sample C has been modeled, as described in Ref. 27, to associate a value of F with each value of V_G. A FN plot at 0 and at 14 T for sample C is shown in Fig. 6; the value of V_G associated with each inverse field tic mark is also given. At 0 T the modulation of the FN plot due to resonant FN tunneling is seen. The dotted line is the least-squares fit of the data for $0.8\times10^{-5} \lesssim 1/F \lesssim 1.4\times10^{-5}$ cm/V. The solid line is ex-

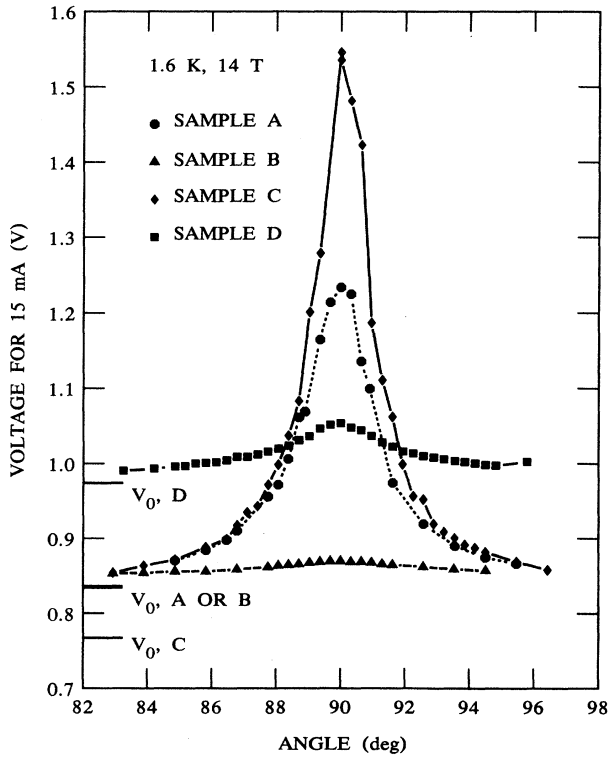

FIG. 3. Dependence of voltage for 15 mA of tunnel current, V_M, on angle between B and J for four samples. $B=14$ T. V_0 is the voltage for 15 mA when $\theta=0°$.

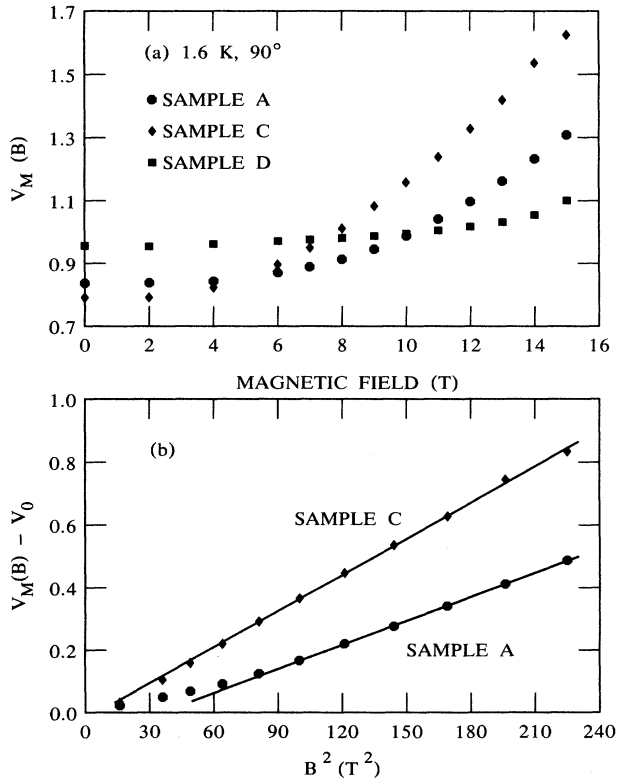

FIG. 4. (a) Dependence of $V_M(B)$ when $\theta=90°$ on B for three samples. (b) Dependence of excess voltage for 15 mA, $V_M(B)-V_0$, on B^2 for samples A and C.

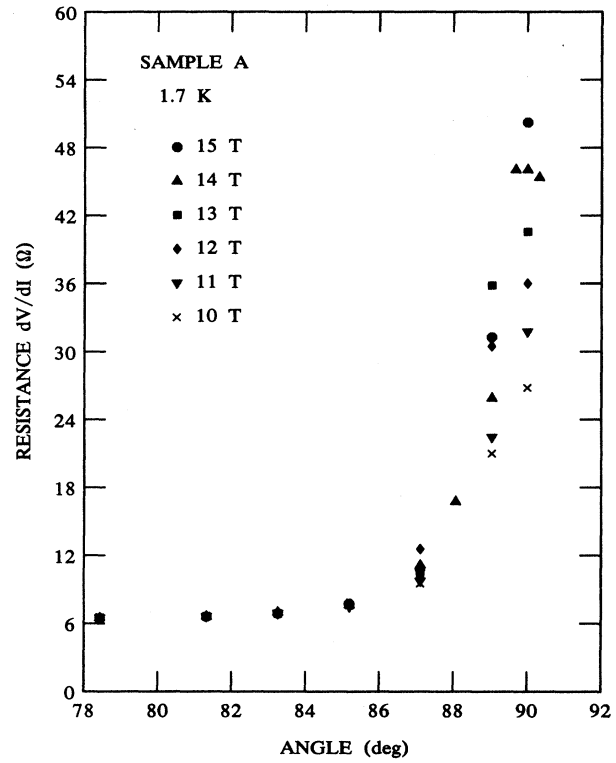

FIG. 5. Dependence of equivalent series resistance dV/dI when $I=15$ mA, on angle for different values of B.

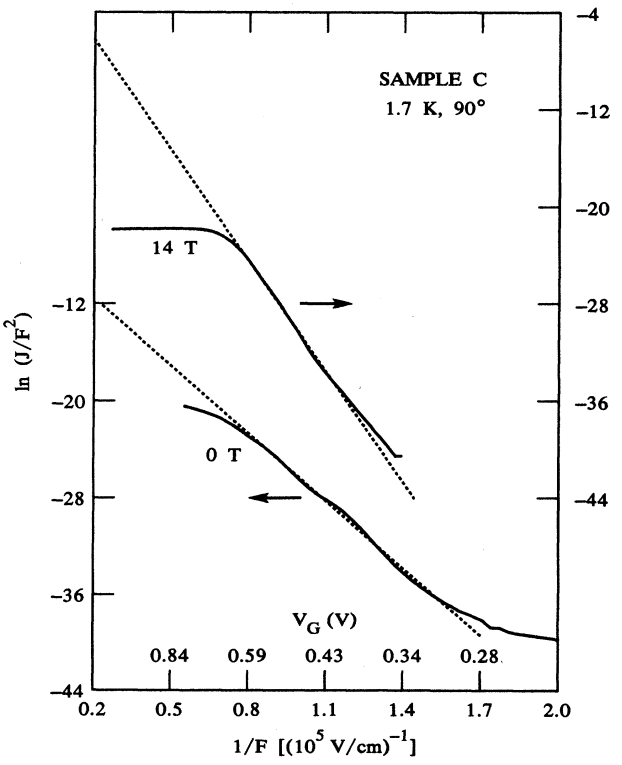

FIG. 6. Fowler-Nordheim plot of I-V curves for sample C at 0 and 14 T. V_G shows voltage for fields corresponding to the tic marks. Solid line is experimental, dotted line is least-squares fit of data for $0.8\times10^{-5}\lesssim 1/F\lesssim 1.4\times10^{-5}$ cm/V.

perimental data. For $1/F\lesssim 0.8\times10^{-5}$ cm/V the values of J/F^2 deviate from the linear FN plot, presumably because of the series resistance of the n^--type GaAs substrate. At 14 T there is still a modulation of I-V curves due to resonant FN tunneling; at high fields J/F^2 is essentially constant. The maximum field for the I-V curve at 14 T of Figs. 1 or 2, corresponding to $J=44$ A/cm^2, is 3.7×10^5 V/cm. If the dotted line through the $B=0$ T FN curve of Fig. 6 is extrapolated to the same field, the current is 4×10^5 A/cm^2, a factor of 9300 higher than the current actually measured at 14 T. Clearly there is a remarkably large reduction of tunnel current for sample C by a transverse magnetic field. The reduction is less for the other three samples but is still substantial.

DISCUSSION

Four aspects of the experimental results on the angular dependence of transverse magnetotunneling at high current densities are of greatest significance: (1) The dependence of V_M on angle is remarkably sharply peaked when θ is varied around 90°. (2) The magnitude of V_M is smaller for samples with larger N_S but the FWHM of the peak is unchanged. (3) The effect of angle is of general occurrence irrespective of whether samples exhibit direct tunneling or FN tunneling, and is independent of parameters of the AlGaAs capacitors except for N_S. (4) For $\theta=90°$, the magnitude of V_M-V_0 is proportional to B^2.

To try to understand these observations qualitatively, consider the schematic band diagram of an accumulation layer on n^--type GaAs in Fig. 7. An accumulation layer for lower substrate doping is shown in Fig. 7(a), for higher substrate doping in Fig. 7(b). An accumulation layer is characterized by a sequence of electric subbands $E_0, E_1, \ldots, E_i$, that are due to the electron confinement by the potential well caused by the field F at the GaAs/$Al_xGa_{1-x}As$ interface. The band bending ψ_S increases as F increases in order to accommodate the increase in the number of electrons in the accumulation layer. At $B=0$ T the density of states in each subband is constant; the energy of all electrons in the direction perpendicular to the interface in a given subband is constant. Weinberg[24,25] and Krieger and Swanson[26] have considered the tunneling of electrons from an accumulation layer on silicon in MOS structures. Weinberg has shown that the factor B_0 in Eq. (2) is nearly the same for an accumulation layer as it would be if tunneling were from a metal. The factor β in Eq. (2) has the same form for FN tunneling from MOS or metal-insulator-metal capacitors.

A number of theoretical calculations of the shape of an accumulation layer on n^--type GaAs, and of the subband separation, have been made.[37–41] The measured substrate doping N_S in Table I is equal to N_D-N_A, where N_D is the number of donors and N_A is the number of acceptors per cm^3 in the substrate. Stern and Das Sarma[38] and Ando[37] have calculated subband separations and the properties of an accumulation layer on n^--type GaAs as the limiting case of an inversion layer. The properties they calculate depend primarily on N_A which is difficult to determine accurately. The compensation ra-

tio $K=N_A/N_D$ also plays a major role in determining conduction in the region of the n^--type GaAs substrate that is not affected by the accumulation layer.[42,43]

For a given interface electron concentration N_I, the accumulation layer extends deeper into the substrate for smaller N_S and N_A. E_0-E_C is smaller and so are $E_1-E_0, E_2-E_1, \ldots$. For the lowest subband the separation of the maximum charge from the interface is between 6 and 10 nm depending on N_A; for higher subbands the wave function spreads out substantially more. For a given N_I more subbands are occupied if N_S and N_A are small. For higher values of N_S, N_D, and N_A, shown schematically in Fig. 7(b), the accumulation layer penetrates less deeply into the substrate, subband separations are larger, and fewer subbands are occupied at high surface electron concentrations. In a magnetic field electrons describe cyclotron orbits whose diameters are $L=2\sqrt{(2i+1)}\sqrt{\hbar/qB}$, where i is the subband index. The solid lines in Fig. 7 show the cyclotron orbit diameters for $\theta=90°$, $i=0$, and three different magnetic fields. Under the high current conditions for which the angular effect is observed, N_I exceeds 10^{12} cm^{-2}. The Fermi level is well into the first excited subband E_1, and may be in higher subbands if they are present. For high B and low N_S the cyclotron orbit becomes smaller than the depth of the accumulation layer; electrons at the Fermi level are confined to paths parallel to and displaced from the interface. The number of electrons that strike the interface with a velocity component perpendicular to the interface is sharply reduced. From Eq. (1) the tunnel current depends on the number of electrons that impinge on the interface that are moving perpendicular to the interface $N(E_z)$ and on a transmission probability $D(E_z)$. The factors on which $D(E_z)$ depend, F, m_I, and ϕ_E, are not functions of angle for $\theta\sim 90°$. However, a reduction of the number of electrons that move perpendicular to the interface can sharply reduce $N(E_z)$ and thus the tunnel current. As θ goes slightly off 90°, the orbit trajectory changes, the number of collisions of electrons with the boundaries of the potential walls increases, and more electrons have a velocity component perpendicular to the interface. In such a case, the number of electrons that can tunnel increases and the value of V_M goes down.

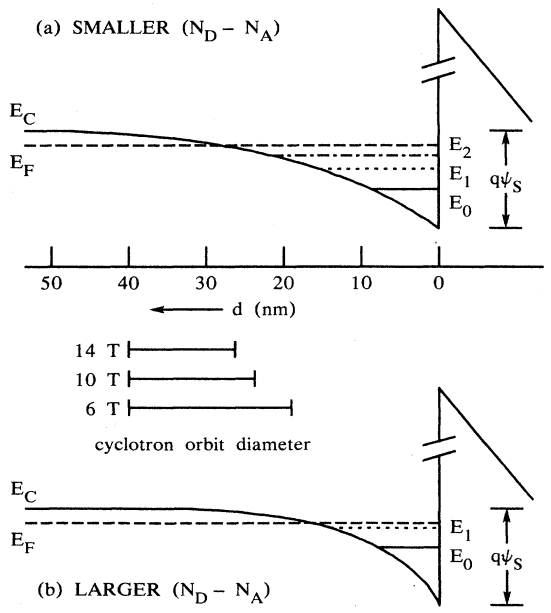

FIG. 7. Schematic band diagram of an accumulation layer on n^--type GaAs for (a) smaller values of N_S. (b) Larger values of N_S. Lines show diameter of cyclotron orbits for different magnetic fields.

Thus, for the schematic model of Fig. 7 increasing N_S has two effects; the number of scattering centers is proportional to N_S, and the number of acceptors N_A, which determine the shape of the accumulation layer, increases as N_S increases. As N_A increases the depth of the accumulation layer decreases and the displacement of electrons from the n^--type GaAs/$Al_xGa_{1-x}As$ interface in high magnetic fields decreases. It is then necessary to go to higher B before the dependence of V_M on angle can be observed.

In Fig. 4 $(V_M-V_0)\propto B^2$ for high values of B parallel to the interface. In the presence of a magnetic field parallel to the interface the energy of subbands is given by

$$E=E_i+(qB)^2\frac{(\langle z^2\rangle_{av}-\langle z_{av}^2\rangle)}{2m_s}, \tag{4}$$

where E_i is the energy of the bottom of the ith subband at 0 T, m_s is the effective mass in the substrate, and $(\langle z^2\rangle_{av}-\langle z_{av}^2\rangle)$ is the square of the standard deviation of the position of the electron normal to the interface.[44] The higher the subband number the greater $(\langle z^2\rangle_{av}-\langle z_{av}^2\rangle)$ is and the greater the amount the band is pushed up by B. In addition, as E_i increases the wave function spreads further, reducing even more the occurrence of collisions that increase the number of electrons that can tunnel in the z direction. Thus the parabolic dependence of (V_M-V_0) on B^2 may be determined by the shift of subbands by B.

The behavior of I-V curves in Figs. 1 and 2 at high B when $\theta=90°$ resembles that which would occur if there were a large resistor in series with the capacitor formed by accumulation layer, $Al_xGa_{1-x}As$ dielectric, and n^+ gate. Magnetic freezeout or magnetic localization of electrons in the bulk of the n^--type GaAs substrate could provide such a series resistance.[42,43] However, the series resistance due to localization is essentially independent of angle for $0°\le\theta\le 90°$. The strong angular dependence of the effective series resistance shown in Fig. 5 is not compatible with its being due to magnetic localization in the substrate which is the mechanism responsible for the increase in series resistance of sample A as B increases.

Thus the schematic model of Fig. 7, in which the effect of N_S on the angular dependence of V_M in Fig. 3 is due to the greater extent of the accumulation layer for small N_S is in qualitative agreement with experiment. Quantitative comparison of theory and experiment requires a knowledge of N_A for a particular sample as well as calcu-

lations of the corresponding properties of an accumulation layer on n^--type GaAs, and of scattering of electrons in an accumulation layer. Even if the detailed mechanisms responsible for the dependence of I-V curves on angle at high current densities are not understood, it provides an accurate electrical method of aligning an AlGaAs capacitor parallel to a magnetic field.

ACKNOWLEDGMENTS

This work would not have been possible without access to F. F. Fang's superconducting magnet. Samples *A*, *C*, and *D* were grown by H. Morkoç, sample *B* by S. L. Wright. M. Heiblum carefully read the manuscript.

[1]T. W. Hickmott, P. M. Solomon, F. F. Fang, R. Fischer, and H. Morkoç, in *Proceedings of the Seventeenth International Conference on the Physics of Semiconductors,* edited by J. D. Chadi and W. A. Harrison (Springer-Verlag, New York, 1985), p. 417.
[2]T. W. Hickmott, Phys. Rev. B **32**, 6531 (1985).
[3]L. Eaves, P. S. S. Guimares, B. R. Snell, F. W. Sheard, D. C. Taylor, G. A. Toombs, J. C. Portal, L. Dmowski, K. E. Singer, G. Hill, and M. A. Pate, Superlatt. Microstruct. **2**, 49 (1986).
[4]P. Guéret, A. Baratoff, and E. Marclay, Europhys. Lett. **3**, 367 (1987).
[5]T. W. Hickmott, Solid State Commun. **63**, 371 (1987).
[6]F. W. Sheard, L. Eaves, and G. A. Toombs, Phys. Scr. T **19**, 179 (1987).
[7]B. R. Snell, K. S. Chan, F. W. Sheard, L. Eaves, G. A. Toombs, D. K. Maude, J. C. Portal, S. J. Bass, P. Claxton, G. Hill, and M. A. Pate, Phys. Rev. Lett. **59**, 2806 (1987).
[8]J. K. Jain and S. Kivelson, Phys. Rev. B **37**, 4111 (1988).
[9]J. A. Lebens, R. H. Silsbee, and S. L. Wright, Phys. Rev. B **37**, 10 308 (1988).
[10]E. Böckenhoff, K. von Klitzing, and K. Ploog, Phys. Rev. B **38**, 10 120 (1988).
[11]L. Brey, G. Platero, and C. Tejedor, Phys. Rev. B **38**, 9649 (1988).
[12]P. A. Shulz and C. Tejedor, Phys. Rev. B **39**, 11 187 (1989).
[13]E. E. Mendez, L. Esaki, and W. I. Wang, Phys. Rev. B **33**, 2893 (1986).
[14]R. A. Davies, D. J. Newson, T. G. Powell, M. J. Kelly, and H. W. Myron, Semicond. Sci. Technol. **2**, 61 (1987).
[15]B. Movaghar, Semicond. Sci. Technol. **2**, 185 (1987).
[16]V. J. Goldman, D. C. Tsui, and J. E. Cunningham, Phys. Rev. B **35**, 9387 (1987).
[17]M. L. Leadbetter, L. Eaves, P. E. Simmonds, G. A. Toombs, F. W. Sheard, P. A. Claxton, G. Hill, and M. A. Pate, Solid-State Electron. **31**, 707 (1988).
[18]F. Ancilotto, J. Phys. C **21**, 4657 (1988).
[19]S. Ben Amor, K. P. Martin, J. J. L. Rascol, R. J. Higgins, A. Torabi, H. M. Harris, and C. J. Summers, Appl. Phys. Lett. **53**, 2540 (1988).
[20]K. K. Choi, B. F. Levine, N. Jarosik, J. Walker, and R. Malik, Phys. Rev. B **38**, 12 362 (1988).
[21]P. England, J. R. Hayes, M. Helm, J. P. Harbison, L. T. Florez, and S. J. Allen, Jr., Appl. Phys. Lett. **54**, 1469 (1989).
[22]C. B. Duke, *Tunneling in Solids* (Academic, New York, 1969), p. 32.
[23]T. W. Hickmott, Phys. Rev. B **39**, 5198 (1989).
[24]Z. A. Weinberg, Solid-State Electron. **20**, 11 (1977).
[25]Z. A. Weinberg, J. Appl. Phys. **53**, 5052 (1982).
[26]G. Krieger and R. M. Swanson, J. Appl. Phys. **52**, 5710 (1981).
[27]T. W. Hickmott, P. M. Solomon, R. Fischer, and H. Morkoç, Appl. Phys. Lett. **44**, 90 (1984).
[28]K. H. Gundlach, Solid-State Electron. **9**, 949 (1986).
[29]J. Maserjian, J. Vac. Sci. Technol. **11**, 996 (1974).
[30]G. Lewicki and J. Maserjian, J. Appl. Phys. **46**, 3032 (1975).
[31]D. J. DiMaria, M. V. Fischetti, J. Batey, L. Dori, E. Tierney, and J. Stasiak, Phys. Rev. Lett. **57**, 3213 (1986).
[32]J. R. Hayes, P. England, and J. P. Harbison, Appl. Phys. Lett. **52**, 1578 (1988).
[33]T. W. Hickmott, P. M. Solomon, R. Fischer, and H. Morkoç, J. Appl. Phys. **57**, 2844 (1985).
[34]J. M. Langer, C. Delerue, M. Lannoo, and H. Heinrich, Phys. Rev. B **38**, 7723 (1988).
[35]T. W. Hickmott, Phys. Rev. B (to be published).
[36]T. W. Hickmott, Phys. Rev. Lett. **57**, 751 (1986).
[37]T. Ando, J. Phys. Soc. Jpn. **51**, 3893 (1982).
[38]F. Stern and S. Das Sarma, Phys. Rev. B **30**, 840 (1984).
[39]M. Tomak and V. E. Godwin, Phys. Status Solidi B **137**, 183 (1986).
[40]D. H. Ehlers and D. L. Mills, Phys. Rev. B **34**, 3939 (1986).
[41]H. Übensee, G. Paasch, D. Bundfuss, and J.-P. Zöllner, Phys. Status Solidi B **148**, 421 (1988).
[42]B. I. Shklovskii and A. L. Efros, *Electronic Properties of Doped Semiconductors* (Springer-Verlag, New York, 1984).
[43]T. W. Hickmott, Phys. Rev. B **38**, 12 404 (1988).
[44]T. Ando, A. B. Fowler, and F. Stern, Rev. Mod. Phys. **54**, 437 (1982).